Dear author,

In the stage of preparing your full work for evaluation, after receiving approval of the corresponding abstract, we kindly ask you to follow the next steps:

1. Update your approved abstract (you might want to introduce modifications) and submit it now in a written version according to the abstract template (many abstracts were introduced directly into the websystem). This version of the abstract will compose the *abstracts booklet* to be distributed to the participants when registering;

2. Fill the form in the next page, indicating to which section you would like your work to be directed. This will help organizing the sessions according to the mini-symposia advertised rather than in the areas and subareas present in the websystem. We apologize for this possible confusion. The reason is that we are using the websystem provided by ABCM, which does not allow us to introduce thematic sessions freely.

If any doubts arise, please contact us.

Your presence in MecSol 2017 will help making this a very successful event. We look forward to seeing you in Joinville!

With kind regards,

The Organizing Committee
MecSol 2017

6th International Symposium on Solid Mechanics

Click on the box to select the Mini-Symposia:

☒ Multiaxial and Fretting Fatigue (*Edgar Mamiya* and *Lucival Malcher*);

☐ Composite Materials (*Ricardo de Medeiros*);

☐ Constitutive Models I – Plasticity and Damage (*Lucival Malcher*, *Miguel Vaz Jr.* and *Edgar Mamiya*);

☐ Constitutive Models II – Viscoelastic and Viscoplastic Solids: Models and Applications (*Heraldo Mattos*);

☐ Impact Engineering (*Marcílio Alves*);

☐ Structural Reliability Methods and Reliability-Based Design Optimization (*André Beck*);

☐ Topology Optimization of Multifunctional Materials, Fluids and Structures (*Eduardo Lenz Cardoso* e *Emilio Carlos Nelli Silva*);

☐ Topological Derivatives: Theory and Applications (*André Novotny*);

☐ X-FEM, G-FEM and Meshfree Methods (*Roberto Dalledone Machado* and *Rodrigo Rossi*);

☐ High Order Finite Elements (*Marco Lúcio Bittencourt*);

☐ Nonlinear Analyses (*Eduardo Campello*);

☐ Other section;

MECSOL Joinville 2017

April 26-28, 2017
Joinville, Santa Catarina, Brazil

Axial-Torsion Testing and Modeling of Fatigue in Extruded AZ31B Magnesium Alloy

Fábio Comes de Castro
Department of Mechanical Engineering
University of Brasilia
fabiocastro@unb.br

Lucival Malcher
Department of Mechanical Engineering
University of Brasilia
malcher@unb.br

Edgar Nobuo Mamiya
Department of Mechanical Engineering
University of Brasilia
mamiya@unb.br

ABSTRACT

The Lemaitre damage model is evaluated using fatigue test data from extruded AZ31B magnesium alloy. The experimental data were obtained from thin-walled tubular specimens subjected to tension–compression, torsion, proportional axial-torsion, and 90º out-of-phase axial-torsion. The Lemaitre model has a difficulty to correlate the data under cyclic torsion loading. A modified Lemaitre model, where the damage denominator depends on the stress triaxiality, correlates well all test data. A simple and fast method is described for determining the material constants in the model.

Keywords: magnesium alloy, multiaxial fatigue, fatigue life, crack initiation

1 INTRODUCTION

Wrought magnesium (Mg) alloys are attractive materials for the automotive and aircraft industries due to their ultra-lightweight, high specific strength, and superior mechanical properties. Structural components in vehicles are often under cyclic loading, and the avoidance of fatigue failure is a critical design consideration. Thus, an understanding of the fatigue behavior of wrought Mg alloys is needed before they can be reliably applied in practice.

Multiaxial fatigue of wrought Mg alloys have not yet been extensively studied. Most of the experiments reported in the literature [1–7] were conducted on thin-walled tubular specimens under constant-amplitude strain-controlled axial-torsion loading. The Mg alloys studied include extruded magnesium–lithium, AZ61A, AZ31B, and AM30. Castro and Jiang [8] have recently investigated the multiaxial fatigue behavior of extruded AZ31B using constant amplitude loading and step loading experiments under both stress- and strain-controlled conditions. A common conclusion found in these studies is that the classical critical plane and energy-based approaches predict reasonably well the

fatigue lives of wrought Mg alloys. Furthermore, the accuracy of the fatigue life prediction is comparable with that obtained for conventional metallic materials tested under similar loading conditions.

The damage model developed by Lemaitre [9] can describe various damage behaviors. Although widely used to estimate ductile fracture, fatigue life prediction based on the Lemaitre model has received much less attention. A recent study [10] indicated that fatigue lives of three conventional metallic materials (304 and S460N steels and 6061-T6 Al alloy) under proportional and nonproportional, axial-torsion loading are correlated reasonably well by the Lemaitre model.

The purpose of this work is to investigate how well fatigue lives can be predicted for an extruded AZ31B Mg alloy using the Lemaitre model. Strain-controlled axial-torsion experiments taken from Ref. [4] were employed in the evaluation. A simple and fast method is described for determining the material constants in the Lemaitre model.

2 MATERIAL AND EXPERIMENTS

Available fatigue tests [4] conducted on an AZ31B Mg alloy were used in the current study. The material was supplied in the form of extruded round bars. The Young's modulus of the material is 44.8 GPa, the shear modulus is 16.9 GPa, the 0.2% offset yield stress in tension is 244 MPa, and the ultimate strength under tension is 298 MPa. Thin-walled tubular specimens were machined from the as-received bars with the longitudinal axes along the extrusion direction. Strain-controlled fatigue experiments were conducted at room temperature using an Instron axial–torsion servohydraulic load frame. The experiments were conducted until the moment when the maximum stress in a loading cycle dropped below 5% of the stabilized or peak value, or a visible crack was found on the outer surface of the specimen. In most cases, a macroscopic surface crack was detected at the end of the test.

The loading paths used in the fatigue tests are shown in Fig. 1. Fully reversed tension–compression, fully reversed torsion, proportional loading, and 90° out-of-phase loading were investigated. During each fatigue test, the axial and shear strains on the outer surface of the specimen were directly measured with a biaxial extensometer, while the axial force and the torque applied to the specimen were measured with the load cells of the machine. At each predefined loading cycle, the strains, the axial force, and the torque were recorded for a minimum of 200 data points. Averaged axial and shear stresses were calculated from the measured loads by assuming uniform axial and shear stress distributions over the wall thickness. In the calculation procedure, the cross-section dimensions during the test were determined considering the elastic deformation and plastic incompressibility of the material.

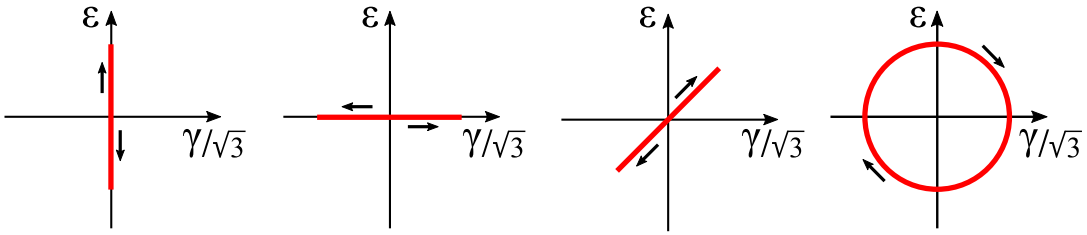

Figure 1. Loading paths used in the fatigue tests.

3 LEMAITRE MODEL

Lemaitre [9] developed a fatigue model for general multiaxial loading based on the framework of continuum thermodynamics. A scalar quantity D is used to describe the fatigue damage at a given material point. Failure is predicted to occur when the fatigue damage reaches a critical value, D_{c}. The damage evolution rule takes the following form:

$$\dot{D} = \left(\frac{Y}{S}\right)^{s} \dot{p} \tag{1}$$

where S and s are material constants and the superposed dot denotes differentiation with respect to time. The quantity $\dot{p}$ is the equivalent plastic strain rate defined as $\dot{p} = \sqrt{2/3}||\dot{\boldsymbol{\varepsilon}}^{\mathrm{p}}||$, where $\boldsymbol{\varepsilon}^{\mathrm{p}}$ is the plastic strain tensor and the symbol $||\ ||$ stands for the Euclidean norm of second-rank tensors. Y is expressed as

$$Y = \frac{\sigma_{\mathrm{eq}}^2 R_\nu}{2E(1-D)^2} \tag{2}$$

In Eq. (2), E is the Young's modulus, σ_{eq} is the von Mises equivalent stress, and R_ν is a scalar function defined as

$$R_\nu = \frac{2}{3}(1+\nu) + 3(1-2\nu)\eta^2 \tag{3}$$

where ν is the Poisson's ratio. The quantity η is called stress triaxiality and is defined as $\eta = \sigma_{\mathrm{h}}/\sigma_{\mathrm{eq}}$, where σ_{h} is the hydrostatic stress.

The original Lemaitre model has a difficulty to correlate the AZ31B test data under tension–compression and torsion, as will be shown in a later section. A simple way to overcome this drawback is to relate the material constant S to the stress triaxiality using a linear relationship,

$$S(\eta) = 3(S_{0.33} - S_0)|\eta| + S_0 \tag{4}$$

where S_0 and $S_{0.33}$ are material constants.

3.1 Constant amplitude loading

The Lemaitre model is applicable to general multiaxial loading. For any loading history, the accumulated fatigue damage can be obtained by numerical integration of Eq. (1). For constant amplitude loading, the stabilized stress and strain responses can be used to evaluate the fatigue damage, and a convenient expression for fatigue life prediction can be derived as follows. The fatigue damage increment per loading cycle is given by

$$\frac{\delta D}{\delta N} = \int_{\mathrm{cycle}} \dot{D}\, \mathrm{d}t \tag{5}$$

Inserting (1) and (2) in (5), and neglecting the variation of D over a cycle, we have

$$\frac{\delta D}{\delta N} = \frac{1}{(1-D)^{2s}} \int_{\text{cycle}} \left(\frac{\sigma_{\text{eq}}^2 R_v}{2ES} \right)^s \mathrm{d}p \tag{6}$$

From the above relation, it follows that

$$(1-D)^{2s} \delta D = I \delta N \tag{7}$$

where

$$I = \int_{\text{cycle}} \left(\frac{\sigma_{\text{eq}}^2 R_v}{2ES} \right)^s \mathrm{d}p \tag{8}$$

The estimated number of cycles to failure, N_{est}, is determined by integrating Eq. (7) over the whole loading history. When the stress and strain responses stabilize well before half the number of cycles to failure, the value of I can be regarded as a constant. Thus, we have

$$\int_0^{D_{\text{c}}} (1-D)^{2s} \delta D = \int_0^{N_{\text{est}}} I \delta N = I N_{\text{est}} \tag{9}$$

In view of (9), the following formula for fatigue life prediction can be obtained:

$$N_{\text{est}} = \frac{1-(1-D_c)^{1+2s}}{(1+2s)I} \tag{10}$$

3.2 Determination of material constants

There are three fatigue-related constants (S, s, D_{c}) in the original Lemaitre model and four constants (S_0, $S_{0.33}$, s, D_{c}) in its modified version based on Eq. (4). To determine these constants, the objective function that is minimized is based on the squared difference between estimated and observed fatigue lives:

$$E = \sum_{i=1}^{n} \left(\log \frac{N_{\text{est}}^{(i)}}{N_{\text{obs}}^{(i)}} \right)^2 \tag{11}$$

where n is the number of test data used to determine the material constants, the superscript (i) denotes the ith test, $N_{\text{obs}}^{(i)}$ is the observed fatigue life, and $N_{\text{est}}^{(i)}$ is the fatigue life estimated by using Eq. (10). To solve the minimization problem, an exhaustive search over a pre-defined domain of candidate constants is carried out. The method can be readily implemented in a computer and its computational cost is very low.

4 RESULTS

Fatigue lives were calculated by using Eq. (10). The stabilized stress–strain hysteresis loops were taken from the fatigue experiments at approximately half the observed fatigue lives. The constants in the original Lemaitre model and in its modified version were determined by best fitting the tension–compression and torsion data, as described in Section 3.2. The fatigue-related constants used in the models are listed in Table 1. The Young's modulus and the Poisson's ratio for the AZ31B Mg alloy are $E = 44.8$ GPa and $\nu = 0.33$, respectively.

Table 1 Material constants used in the fatigue models

Original Lemaitre model	Modified Lemaitre model
$S = 1.4$	$S_0 = 0.6$, $S_{0.33} = 1$
$s = 2.2$	$s = 2.8$
$D_c = 0.3$	$D_c = 1$

Estimated lives based on the original Lemaitre model and the observed lives are compared in Fig. 2. A data point with a horizontal arrow denotes a run-out test. It is seen that the original Lemaitre model is not capable to line up the tension–compression and torsion data. This result reveals a drawback in the original model, since the capacity of a fatigue model to satisfactorily correlate tension–compression and torsion data serves as a basic benchmark to critically evaluate a given model. The results in Fig. 2 also show a loss of accuracy in the fatigue life estimates for lives higher than 5 × 10^5 cycles. The difficulty in accurately measuring small plastic strains at long fatigue lives may have contributed to such less desirable predictions. Since the damage increment in the Lemaitre model is driven by the plastic strain increment, the estimated fatigue life is affected by inaccuracies in the plastic strains.

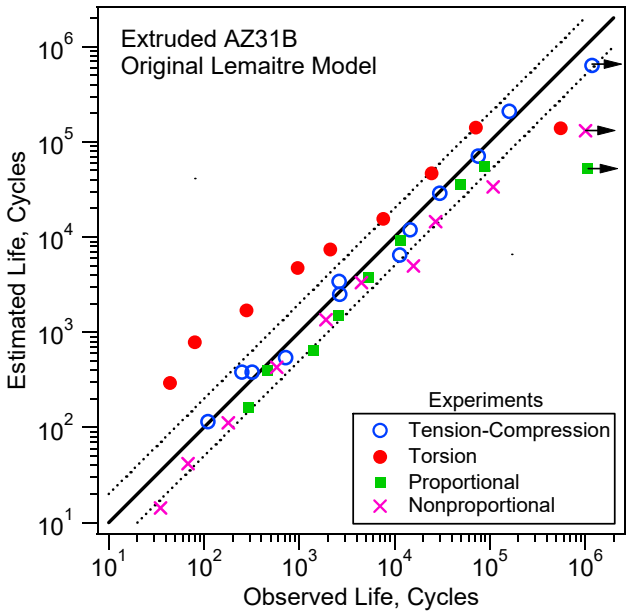

Figure 2: Observed life versus estimated life based on the original Lemaitre model.

Figure 3 shows the fatigue lives predicted by the modified Lemaitre model versus the observed fatigue lives. The baseline tension–compression and torsion data were within the factor-of-two boundaries in fatigue life, the only exception being the torsion test that failed with $N_f = 556{,}020$ cycles. A significant improvement in the correlation of the baseline data was obtained as compared to the original model (cf. Fig. 2) and this is due to the assumption that S is a function of the stress triaxiality. For fatigue lives below 5×10^5 cycles, the predicted fatigue lives for the proportional and nonproportional tests are generally within the factor-of-three boundaries, indicating a reasonable fatigue life prediction. Again, the loss of accuracy in the life estimates for the high-cycle fatigue tests ($N_f > 5 \times 10^5$ cycles) is possibly due to inaccuracies in the measured plastic strains.

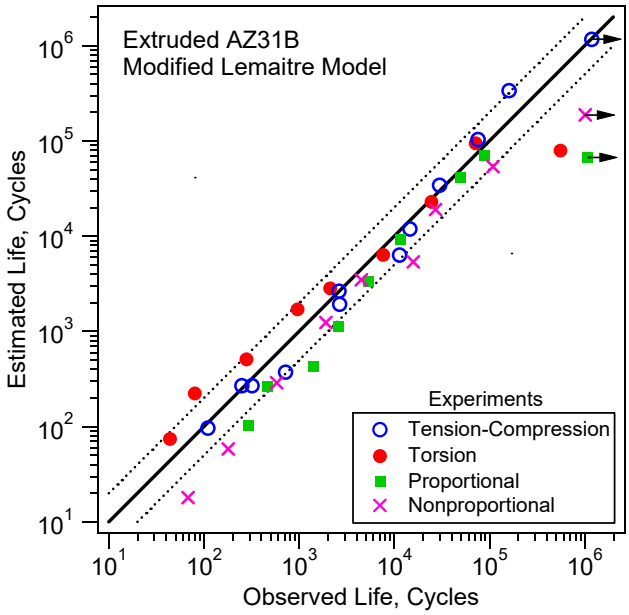

Figure 3: Observed life versus estimated life based on the modified Lemaitre model.

The limited stress states that were employed to evaluate the modified Lemaitre model may have contributed to its good correlation of the fatigue lives. Thin-walled tubular specimens under axial-torsion loading inherently experience limited values of stress triaxiality. Figure 4 shows the variation of the stress triaxiality with normalized time for selected proportional and nonproportional tests. Since identical variations of the stress triaxiality were observed in the other tests, they were omitted from Fig. 4. It is seen that the stress triaxiality for the tests in Fig. 4 lies in the range $0 \leq |\eta| \leq 1/3$. This is in fact a feature of any axial-torsion stress state because whenever $\sigma \neq 0$ the denominator of the expression for the stress triaxiality, $\eta = 1/3\ \sigma/\sqrt{\sigma^2 + 3\tau^2}$, is always equal or greater than $|\sigma|$. Since the constants in the modified Lemaitre model were determined by using fatigue data with $\eta = 0$ (torsion tests) and $|\eta| = 1/3$ (tension–compression tests), this may have contributed to the good life estimates. Fatigue experiments covering a wide range of stress triaxiality are needed to better evaluate the modified Lemaitre model.

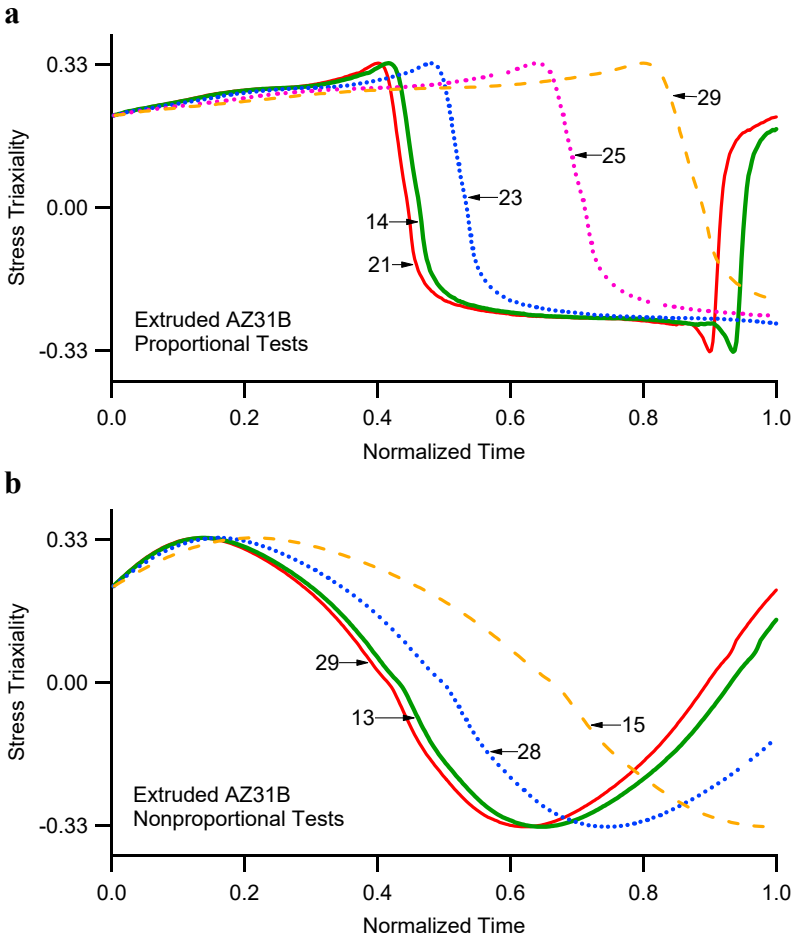

Figure 4: Variation of stress triaxiality, η, with normalized time, t/T, for selected proportional tests (a) and nonproportional tests (b). t denotes a time instant and T is the cyclic load period. The two digits in the annotation for a curve denote the specimen number as defined in Ref. [4].

5 CONCLUSIONS

The Lemaitre damage model was experimentally evaluated using axial-torsion fatigue data of extruded AZ31B Mg alloy. The model has a difficulty to correlate the data under cyclic torsion loading. Fatigue life estimates made with a modified Lemaitre model, where the damage denominator depends on the stress triaxiality, compared well with test data. A simple and effective method was derived for the determination of the materials constants in the fatigue model. Fatigue experiments covering a wide range of stress triaxiality are needed to better evaluate the modified Lemaitre model.

6 ACKNOWLEDGEMENTS

The supports provided by CNPq (contracts 310845/2013-0 and 304083/2013-5) are gratefully acknowledged.

REFERENCES

[1] Bentachfine, S., Pluvinage, G., Toth, L.S., Azari, Z., 1996. Biaxial low cycle fatigue under non-proportional loading of a magnesium–lithium alloy. Eng. Fract. Mech. 54, 513–522.

[2] Yu, Q., Zhang, J., Jiang, Y., Li, Q., 2011b. Multiaxial fatigue of extruded AZ61A magnesium alloy. Int. J. Fatigue 33, 437–447.

[3] Albinmousa, J., Jahed, H., Lambert, S., 2011. Cyclic behaviour of wrought magnesium alloy under multiaxial load. Int. J. Fatigue 33, 1127–1139.

[4] Xiong Y, Yu Q, Jiang Y, (2012), "Multiaxial fatigue of extruded AZ31B magnesium alloy", Materials Science and Engineering: A, 546, 119–128.

[5] Albinmousa, J., Jahed, H., 2014. Multiaxial effects on LCF behaviour and fatigue failure of AZ31B magnesium extrusion. Int. J. Fatigue 67, 103–116.

[6] Castro F, Jiang Y, (2016), "Fatigue life and early cracking predictions of extruded AZ31B magnesium alloy using critical plane approaches", International Journal of Fatigue, 88, 236–246.

[7] Roostaei AA, Jahed H, (2017), "Multiaxial cyclic behaviour and fatigue modelling of AM30 Mg alloy extrusion", International Journal of Fatigue, 97, 150–161.

[8] Castro F, Jiang Y, (2017), "Fatigue of extruded AZ31B magnesium alloy under stress- and strain-controlled conditions including step loading", Mechanics of Materials, Submitted for Publication.

[9] Lemaitre J, Desmorat R, (2005), Engineering Damage Mechanics: Ductile, Creep, Fatigue and Brittle Failures, Springer.

[10] Lopes JP, Malcher L, (2017), "Fatigue life estimates under non-proportional loading through continuum damage evolution law", Theoretical and Applied Fracture Mechanics, Article in Press.

RESPONSIBILITY NOTICE

The authors are the only responsible for the printed material included in this paper.